

Two-Dimensional Shear-Layer Entrainment

Paul E. Dimotakis*

California Institute of Technology, Pasadena, California

It is observed experimentally that a spatially growing shear layer entrains an unequal amount of fluid from each of the freestreams, resulting in a mixed fluid composition that favors the high-speed fluid. A simple argument is proposed, based on the geometrical properties of the large-scale flow structures of the subsonic, fully developed, two-dimensional mixing layer, which yields the entrainment ratio and growth of the turbulent mixing layer. The predictions depend on the velocity and density ratio across the layer and are in good agreement with measurements to date.

I. Introduction

THE concept of entrainment has evolved in recent years with our changing perspective of turbulent flow. As a consequence, one of the difficulties in discussing this topic is that several possible definitions of entrainment exist at present, not necessarily equivalent, assumed either implicitly in discussions and analyses or operationally through particular choices and interpretations of measurements in the laboratory.

In the original discussions of Corrsin and Kistler,¹¹ the turbulent region was envisioned as circumscribed by the superlayer, an interfacial surface of a relatively simple topology, which marked the instantaneous boundary between the turbulent and nonturbulent flow. Within this superlayer, the turbulent region was treated as essentially homogeneous and isotropic. In this context, entrainment could be described as the flux of nonturbulent fluid across the superlayer interface, in turn, the consequence of the random diffusive propagation, as dictated, and augmented, by the local flowfield, of the superlayer into the nonturbulent fluid. (See also related discussions in Refs. 22–24.)

Entrainment by the Corrsin and Kistler mechanism has come to be known as “nibbling” of the irrotational fluid by the rotational (turbulent) fluid. Work in the last fifteen years or so on the structure of turbulent shear flows suggests that this picture may be too simple to provide the conceptual basis for the description of entrainment of nonturbulent irrotational fluid into the turbulence. The term “gulping” has been coined to describe the resulting suggested picture, and it now appears that this process might best be described as possessing three main phases, which can be outlined as follows.

Initially, fluid in the vicinity of the vorticity-bearing fluid is set in motion through the Biot-Savart-induced velocity field. Note that this phase of the process is kinematic and not diffusive. Irrotational fluid sufficiently close to the vortical fluid will in fact participate in the large-scale structure motions long before it has acquired vorticity of its own. This first phase of entrainment could be called *induction* (the term arose out of discussions with Professors A. Roshko and R. Narasimha) and describes largely irrotational fluid that has started at the low end of the turbulent wave-number spectrum and should therefore be considered as part of the turbulent flow. See Fig. 1. Brown and Roshko⁸ identified this “entanglement” stage of entrainment as distinct from the subsequent phases of the

overall process. Inducted fluid, even though still irrotational, is part of the motion in the turbulent region and already contributes to the overall momentum and energy of that region.²¹ It should be emphasized that the *induction velocity* should not be confused with the *induced velocity* corresponding to the Biot-Savart law and the large-scale vorticity concentrations in free shear flows, or with the *displacement velocity* at large distances from the turbulent region.

Secondly, following the induction of irrotational fluid into the turbulent region, a fluid element is strained until its spatial scale is small enough (large wave number) to put it within reach of (viscous) diffusive processes. In this phase, which could be called *diastrophy* or turning ($\sigma\tau\phi\eta$) through ($\delta\alpha^-$) some action or influence, the irrotational fluid is “corrupted” with vorticity through the action of viscosity as it cascades to spatial scales of the order of the viscous (Kolmogorov) scale λ_ν .

A third stage can be associated with other possible diffusive processes, such as molecular mixing or heat conduction, and may or may not precede the second stage, depending on the relative magnitude of the corresponding molecular diffusivity to that of the kinematic viscosity. This third stage, which could be called *infusion*, would of course be almost indistinguishable from the diastrophy phase in the case of gas-phase entrainment, for which the values of the corresponding diffusion coefficients are usually of the same order. In the case of liquid-phase molecular mixing, however, for which Schmidt numbers are of the order of 10^3 , or in the case of the diffusion of particulates and aerosols, for which the effective diffusivity is set by Brownian motion with Schmidt numbers that can reach values of the order of 10^5 – 10^6 , the corresponding diffusion scale λ_D , which differs from the viscous scale by the square root of the Schmidt number, i.e.,

$$\lambda_D = \lambda_\nu \cdot Sc^{-1/2} \quad (1)$$

can be very much smaller and is the species diffusion counterpart of the Batchelor scale.¹ In particular, if we are interested in chemical reactions between the entrained fluids into a turbulent shear layer, this last stage of entrainment is important, and it is this difference between gases and liquids that can result in the large Schmidt number effects on the reaction rates documented recently for the fully developed two-dimensional shear layer between liquid-phase reactions^{4,15} and gas-phase reactions.^{19,26}

It can be seen that for a Schmidt (or Prandtl) number substantially different from unity, as in the case of liquids or particulate dispersal, for example, a different volume fraction would be associated with fluid in each of the three phases. In particular, we would expect that the volume fraction occupied by molecularly mixed fluid in a liquid would be smaller than the volume fraction of vortical fluid. Analogously, depending

Presented as Paper 84-0368 at the AIAA 22nd Aerospace Sciences Meeting, Reno, NV, Jan. 9–12, 1984; received Dec. 13, 1984; revision received April 10, 1986. Copyright © 1986 by P. E. Dimotakis. Published by the American Institute of Aeronautics and Astronautics, Inc., with permission.

*Professor. Member AIAA.

on the monitored property of interest, the corresponding "intermittency" would be different.

II. Experimental Data and Discussion

Measurements by Konrad¹⁴ in a two-dimensional, gas-phase shear layer at high Reynolds numbers show that the entrainment of fluid from the two freestreams into the turbulent mixing layer is not symmetric. Using a small aspirating probe⁷ and ignoring possible correlations between composition and velocity fluctuations, Konrad estimated the flux of mixed fluid, which he defined operationally as fluid whose composition was measurably different from that of either of the pure freestreams. It can be seen, on the basis of the preceding discussion, that whereas Konrad's estimates of the absolute values of the entrainment flux from each of the freestreams correspond to the *infusion* flux and not the *induction* flux, which is higher, his estimate of the entrainment ratio is probably reliable and approximately equal to the induction ratio. The asymmetric entrainment ratio was also appreciated by J. Brown,⁹ who argued for it on the basis of the apparent angles of intersection of the edges of the shear-layer turbulent region and those of the corresponding freestreams.

Confirmation of this entrainment asymmetry can also be found in the measurements by Mungal and Dimotakis¹⁹ at high Reynolds numbers, in a gas-phase chemically reacting shear layer ($H_2 + F_2$), as well as in the laser-induced fluorescence measurements in a liquid-phase chemically reacting shear layer in water by Koochesfahani et al.¹⁸ at a lower Reynolds number and in the dilution experiments of Koochesfahani and Dimotakis,¹⁶ at a higher Reynolds number.

These results may be considered surprising at first sight. In the absence of an imposed streamwise pressure gradient (constant freestream velocities), the large-scale vortical structures in a two-dimensional, shear-layer convect with a constant velocity U_c . Consequently, there exists a Galilean frame translating at U_c , in which the vortices are stationary. In this vortex frame, one will observe the high-speed freestream going in one direction with a speed $U_1 - U_c$ and the low-speed freestream going in the opposite direction with a speed $U_c - U_2$. For equal freestream densities ($\rho_2 = \rho_1$), the convection velocity is found to be approximately equal to the mean speed of the layer $\bar{U} = (U_1 + U_2)/2$. The corresponding freestream velocities, in the vortex rest frame, would then be equal to $\Delta U/2$ and $-\Delta U/2$, respectively, where $\Delta U = U_1 - U_2$ is the velocity difference across the layer. Consequently, for uniform-density flow, it would appear that in the vortex frame the two freestreams provide a symmetric environment.

It is important to recognize that this argument is valid for a *temporally* growing shear layer and, for equal freestream densities ($\rho_2 = \rho_1$), one would therefore conclude that such a layer will entrain equal amounts of fluid from the two freestreams. This has been argued by G. Brown,⁶ who proposed that the entrainment ratio should be equal to the square root of the freestream density ratio.

Konrad's¹⁴ measurements at high Reynolds numbers indicate that the entrainment ratio is a function of both the

freestream speed ratio $r = U_2/U_1$ and the density ratio $s = \rho_2/\rho_1$ across the shear layer. For a uniform-density shear layer ($s = 1$) and a speed ratio of $r \approx 0.38$, Konrad measured a volume flux entrainment ratio of $E_v(r, s) \approx 1.3$. Using a high-speed stream of helium and a low-speed stream of nitrogen, corresponding to a density ratio of $\rho_2/\rho_1 = 7$, and the same speed ratio of 0.38, he measured a volume flux entrainment ratio of $E_v(r, s) \approx 3.4$. It should be noted that, for a fixed-speed ratio r , the ratio of the two (volume flux) entrainment ratios, as measured by Konrad, is approximately in the ratio of the square root of the density ratios, i.e., $E_v(r, s_1) \div E_v(r, s_2) \approx (s_1/s_2)^{1/2}$, consistent with the density dependence of the proposed entrainment ratio expression by G. Brown.⁶

The preceding observations suggest a functional dependence of the (volume) entrainment ratio E_v on the density ratio s and the velocity ratio r of the form

$$E_v(r, s) = \sqrt{s} \cdot f(r) \quad (2)$$

The fact that a temporally growing shear layer at uniform density must be characterized by a symmetric entrainment ratio suggests that the function $f(r)$ in the preceding equation must tend to unity as the velocity ratio r tends to unity, as has been argued by G. Brown.⁶ In turn, Konrad's measurements at uniform density and a velocity ratio of $r \approx 0.38$ suggest the value of $f(0.38) \approx 1.3$, in disagreement with G. Brown's⁶ proposal, which would predict a symmetric entrainment ratio under these conditions.

III. Entrainment into a Spatially Growing Layer

The discussion of entrainment in the spatially growing shear layer is complicated by the coalescence interactions between the large-scale vortex structures, which do not allow a steady flow analysis of the problem. Nevertheless, there is evidence in the Hernan and Jimenez¹³ digital image analysis of the motion picture data of Bernal³ to suggest that the coalescence interactions themselves are not responsible for any significant additional contribution to the entrainment flux. In particular, Hernan and Jimenez find that the visual area of the turbulent region of the structure emerging from the coalescence is very close to the (extrapolated) sum of the areas of the participating structures prior to pairing. Consequently, we are encouraged to consider an approximation of entrainment as a continuous process, briefly interrupted by occasional coalescence interactions. It should be noted, however, that this conjecture is at variance with the suggestion of Winant and Browand,²⁵ who argued, on the basis of their flow visualization experiments in the two-dimensional shear layer, that the pairing process is in fact primarily responsible for entrainment. Of course, in the context of the preceding discussion, it should be recognized that the apparent discrepancy may be semantic, in view of the possible identification, in each case, with a different phase (induction, diastrophy, or mixing) of the entrainment process.

Keeping these issues in mind, we might be able to argue for entrainment in the spatial layer as follows. Consider the n th vortex at x_n in the spatially growing layer, viewed in the vortex rest frame, with the splitter plate trailing edge receding with a velocity $-U_c$ and, at an instant between pairings, its upstream and downstream neighbors at x_{n-1} and x_{n+1} , respectively (see Fig. 2). The ratio of the high-speed fluid induction velocity v_{i1}

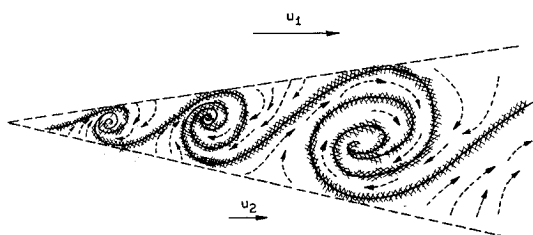


Fig. 1 Entrainment stages. Dashed lines indicate induced fluid (irrotational) velocity field in the vortex frame. Crosshatched fluid indicates vortical (viscous) fluid. Solid line indicates molecularly mixed (high-Schmidt-number) fluid.

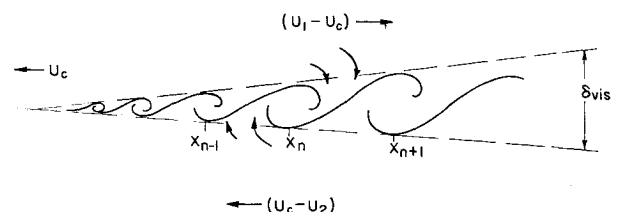


Fig. 2 Large-structure array and induction velocities in vortex convection frame.

to the apparent velocity $U_1 - U_c$ of the high-speed freestream in the vortex frame will, in general, be some function of the dimensionless parameters of the problem, i.e., $-v_{i1}/(U_1 - U_c) = \epsilon_1(r, s)$, and similarly for $v_{i2}/(U_c - U_2) = \epsilon_2(r, s)$.

The ansatz is now proposed that the two dimensionless functions $\epsilon_1(r, s)$ and $\epsilon_2(r, s)$ are equal, i.e.,

$$\frac{-v_{i1}}{U_1 - U_c} = \frac{v_{i2}}{U_c - U_2} = \epsilon(r, s) \quad (3)$$

Note that, consistent with the ansatz, the ratio of the induction velocities $-v_{i1}/v_{i2}$ is equal to the freestream velocity ratio in the vortex frame, i.e., $(U_1 - U_c)/(U_c - U_2)$, or $(1 - r_c)/(r_c - r)$, where $r_c = U_c/U_1$ is the normalized vortex convection velocity and $r = U_2/U_1$ is the freestream speed ratio in the laboratory frame.

Vortex Convection Velocity

To proceed, we need to evaluate the normalized vortex convection velocity which, for equal densities ($s = 1$), is known to be approximately equal to $\bar{r} = (1 + r)/2$, the normalized mean speed of the layer. On the other hand, on the basis of the $x-t$ data in Brown and Roshko,⁸ we find that the normalized convection velocity for a density ratio $s = 7$ and a velocity ratio $r = 0.38$ is in the range of $0.53 < r_c < 0.56$ (vs $\bar{r} = 0.69$ at this velocity ratio).

The vortex convection velocity can be estimated with the aid of the following argument. For a two-dimensional shear layer, and in the Galilean rest frame of the vortices, a stagnation point must exist between them, as was pointed out by Coles.¹⁰ Consequently, Bernoulli's equation would apply along a line through this point and, treating the flow as approximately steady along this line, the dynamic pressures in the two freestreams (in this frame) will be approximately matched. If second-order differences in the static pressure across the layer are ignored, we then have

$$\rho_1(U_1 - U_c)^2 \approx \rho_2(U_c - U_2)^2 \quad (4)$$

which yields the freestream velocity ratio in the frame of the vortices,

$$\frac{1 - r_c}{r_c - r} = s^{1/2} \quad (5)$$

Solving for the normalized convection velocity r_c , we then obtain

$$r_c(r, s) = \frac{1 + rs^{1/2}}{1 + s^{1/2}} \quad (6)$$

The resulting expression for the convection velocity r_c is plotted in Fig. 3. Note that:

- 1) It is linear in the velocity ratio r .
- 2) For equal densities, it predicts a convection velocity equal to the mean speed \bar{r} , i.e., $r_c(r, s = 1) = (1 + r)/2$.
- 3) It gives a value of r_c ($r = 0.38, s = 7$) = 0.55, in good agreement with the Brown and Roshko⁸ $x-t$ data at these conditions.
- 4) The large structure convection velocity U_c exceeds the mean speed of the layer $\bar{U} = (U_1 + U_2)/2$ for a heavy high-speed fluid ($\rho_1 > \rho_2$) and, conversely, is less than the mean speed for a light high-speed fluid ($\rho_2 > \rho_1$), i.e., a heavy high-speed fluid "drags" the vortices along.

Entrainment Ratio

If we now assume that the motion of the entrained fluid can be represented as indicated in Fig. 2, we can argue that the high-speed fluid (volume) induction flux should be propor-

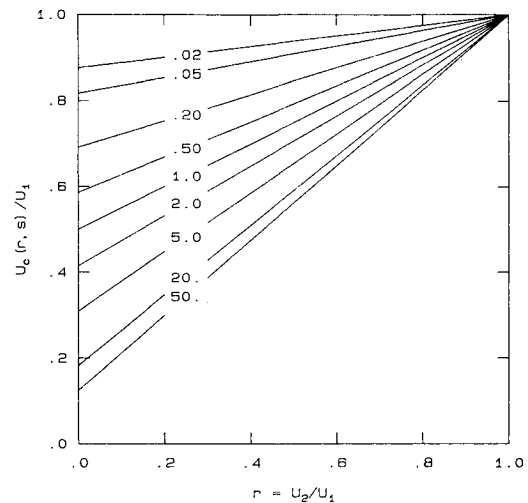


Fig. 3 Normalized vortex convection velocity $U_c(r, s)/U_1$ vs the freestream speed ratio $r = U_2/U_1$. Line labels correspond to selected values of freestream density ratio $s = \rho_2/\rho_1$.

tional to $-v_{i1} \cdot (x_{n+1} - x_n)$, the product of corresponding induction velocity and the chord subtended between the n th vortex and its downstream neighbor, while the low-speed fluid induction flux should be proportional to $v_{i2} \cdot (x_n - x_{n-1})$, the product of the corresponding induction velocity and the chord subtended between the n th vortex and its upstream neighbor. Therefore, using Eq. (3), the volume flux entrainment (induction) ratio E_v should be given by

$$E_v = \frac{U_1 - U_c}{U_c - U_2} \cdot \frac{x_{n+1} - x_n}{x_n - x_{n-1}} \quad (7)$$

Since the $\{x_n\}$ position sequence constitutes a geometric progression, i.e., $x_{n+1} = (1 + \ell/x) \cdot x_n$, we have, combining with Eq. (5),

$$E_v = s^{1/2} [1 + (\ell/x)] \quad (8)$$

where ℓ/x is the (mean) vortex spacing to position ratio, which is a constant of the flow (i.e., $\ell \sim x$).

The ratio ℓ/x can be estimated using the relation suggested by Koochesfahani et al.¹⁶ Based on their cross-correlation measurements, these authors report a value of

$$\ell/x = 3.9(\delta_\omega/x) \quad (9)$$

where δ_ω/x is the vorticity thickness to position ratio, experimentally found to be proportional to $(1 - r)/(1 + r)$ for equal densities ($\rho_2 = \rho_1$), with the constant of proportionality in the range 0.16–0.18 (the higher value is the one recommended by Brown and Roshko⁸). If we substitute the mid-range value for δ_ω/x , we have

$$\frac{\delta_\omega}{x} = 0.17 \frac{1 - r}{1 + r} \quad (10)$$

where $r = U_2/U_1$ is the velocity ratio across the shear layer. Combining the latter two equations yields an expression for ℓ/x , i.e.,

$$\frac{\ell}{x} = 0.68 \frac{1 - r}{1 + r} \quad (11)$$

It should be noted that even though the empirical relations, as given by Eqs. (9) and (10), are based on shear-layer data with equal freestream densities, Konrad's flow visualization data suggest that ℓ/x is not a function of the freestream density ratio. Consequently, we are encouraged to accept Eq. (11) as

valid for all velocity and density ratios, even though expressions (9) and (10) are not.

Substituting this expression for ℓ/x in Eq. (8) then yields, for the entrainment ratio,

$$E_v(r, s) = s^{1/2} \left(1 + 0.68 \frac{1-r}{1+r} \right) \quad (12)$$

Note that the mass flux entrainment ratio E_m can also be obtained from the preceding equation, since $E_m = E_v/s$, or

$$E_m(r, s) = s^{-1/2} \left(1 + 0.68 \frac{1-r}{1+r} \right) \quad (13)$$

The resulting proposed expression for the (volume flux) entrainment ratio [Eq. (12)], is of the form suggested by Eq. (3). For equal densities,

1) The entrainment ratio tends to unity as the velocity ratio tends to unity, i.e., $E(r \rightarrow 1, s=1) \rightarrow 1.0$, in agreement with the temporally growing shear layer, which should approximate this case in the limit.

2) It predicts an excess entrainment of high-speed fluid.

3) For a velocity ratio $r=0.38$, it predicts an entrainment ratio of $E_v=1.31$ (in good agreement with Konrad's measured estimate of 1.3).

4) For a density ratio of $s=7$ and a velocity ratio of $r=0.38$, it predicts an entrainment ratio of $E_v=3.46$ (in good agreement with Konrad's experimental estimate of 3.4).

The function $E_v(r, s)$ of Eq. (12) is plotted in Fig. 4 vs the velocity ratio r , for equal densities ($s=1$), and in Fig. 5 vs the density ratio s , for a velocity ratio $r=0.38$.

Shear-Layer Growth

Viewing the overall entrainment into the layer, the induction velocity ansatz also suggests that the growth of the thickness of the layer, in the vortex frame, should, in the mean, be linear in time. In particular, the induction flux from the two freestreams results in a growth of the area A_n

$$A_n \approx \frac{1}{2} \delta_n (x_{n+1} - x_{n-1})$$

between pairings, with vortex spacings temporarily constant, which we can estimate linearly by

$$\frac{A_n}{t} = \epsilon [(U_1 - U_c)(x_{n+1} - x_n) + (U_c - U_2)(x_n - x_{n-1})] \quad (14)$$

Substituting for A_n , dividing through by x_{n-1} , and rearranging terms, we have

$$\frac{\delta}{t} \left(1 + \frac{\ell}{2x} \right) \approx \left[(U_1 - U_2) \left(1 + \frac{\ell}{x} \right) + (U_c - U_2) \right]$$

where ℓ/x is the vortex-spacing-to-position ratio [see Eq. (11)]. Solving for δ/t then yields

$$\frac{\delta}{t} = \epsilon \left[(U_1 - U_2) - (U_c - \bar{U}) \frac{\ell/x}{1 + \ell/2x} \right]$$

where $\bar{U} = (U_1 + U_2)/2$ is the mean speed of the layer. Transforming back to laboratory coordinates and normalizing all velocities by U_1 (note that $t = x/U_c$), we have

$$\frac{\delta}{x} = \epsilon \left[\frac{1-r}{r_c} - \left(1 - \frac{1+r}{2r_c} \right) \frac{\ell/x}{1 + \ell/2x} \right] \quad (15)$$

For equal densities ($s=1$), the convection velocity is predicted to be equal to the mean speed, i.e., $r_c = \bar{r} = (1+r)/2$, the difference inside the parentheses vanishes, and we recover

the familiar form of shear-layer growth [see Eq. (10)], i.e.,

$$\frac{\delta}{x} = \text{const} \frac{1-r}{1+r} \quad (16)$$

which lends credence to the ansatz of Eq. (3) and suggests that $\epsilon \neq f(r)$, at least for $s \approx 1$. If the latter is also assumed to hold for $s \neq 1$, we obtain a prediction for the growth of the two-dimensional shear layer given by

$$\frac{\delta}{x} = \epsilon \left(\frac{1-r}{1+s^{1/2}r} \right) \left[1 + s^{1/2} - \frac{1-s^{1/2}}{1+2.9(1+r)/(1-r)} \right] \quad (17)$$

where Eqs. (6) and (11) have been used for r_c and ℓ/x , respectively.

The resulting growth law, corresponding to the vorticity (maximum slope) thickness δ_ω/x of Brown and Roshko,⁸ is plotted in Fig. 6 vs $(1-r)/(1+r)$ for $s=1/7, 1$, and 7 , using the value of $2\epsilon_\omega=0.17$ for the corresponding constant from Eq. (10).

Note that the second term in the brackets vanishes as $s \rightarrow 1$ or $r \rightarrow 1$. Note also that if we neglect the second term in the brackets, which arises from the upstream/downstream asymmetry of the spatially growing layer, we recover the shear-

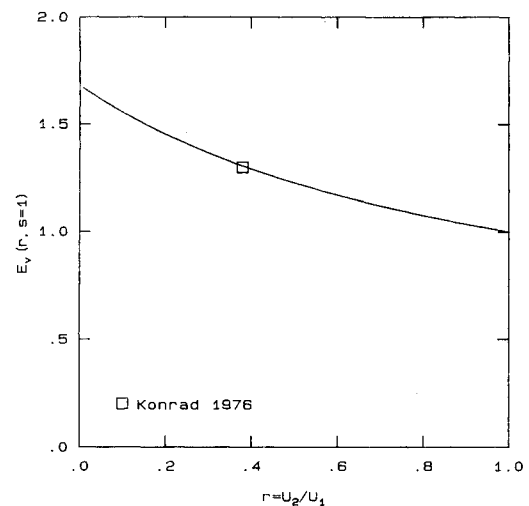


Fig. 4 Volume flux entrainment ratio E_v vs freestream speed $r = U_2/U_1$ for equal freestream densities ($s = \rho_2/\rho_1 = 1$).

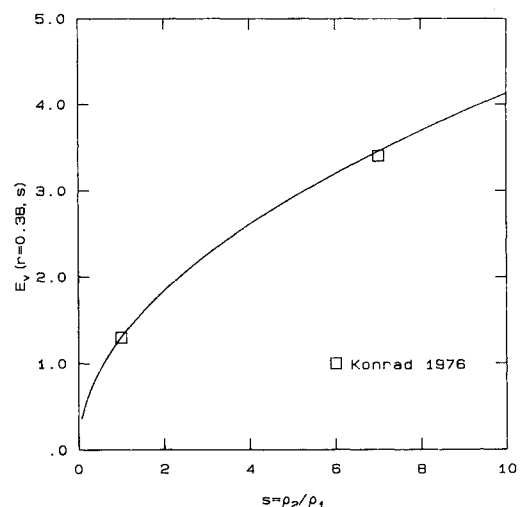


Fig. 5 Volume flux entrainment ratio E_v vs freestream density ratio $s = \rho_2/\rho_1$ for a speed ratio $r = U_2/U_1 = 0.38$.

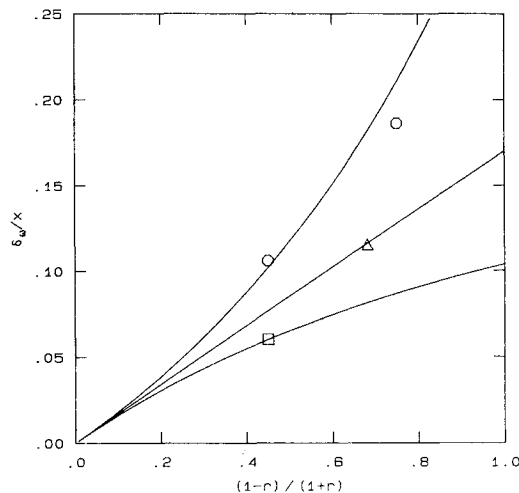


Fig. 6 Vorticity (maximum slope) thickness δ_ω/x for density ratios $s = 1/7, 1$, and 7 . Circle and square data points from Ref. 8 ($s = 7, 1/7$, respectively). Triangle from Ref. 12 ($s = 1$).

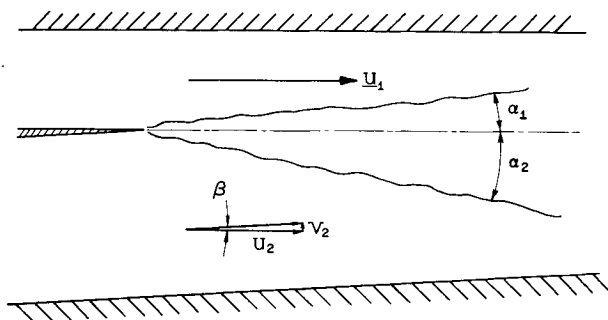


Fig. 7 Shear-layer geometry.

layer growth law proposed by G. Brown,⁶ which should be valid for the temporally growing shear layer (i.e., as $r \rightarrow 1$).

Shear-Layer Orientation

If we could assume that the ratio of induced fluid fluxes from each of the freestreams is also equal to the ratio of the fluid flux crossing the corresponding (mean) visual edges of the shear layer, we could use Eqs. (12) and (17) to estimate the angles subtended between the upper and lower (mean visual) edges of the layer and the direction of the high-speed stream velocity vector, respectively. Aligning the x axis with the U_1 vector, and denoting the corresponding (positive) angles of the high- and low-speed shear-layer edges by α_1 and α_2 , respectively, we have

$$\frac{1}{r} \frac{\tan \alpha_1}{\tan \alpha_2 + \tan \beta} = E_v \quad (18a)$$

$$\tan \alpha_1 + \tan \alpha_2 = \frac{\delta_{vis}}{x} \quad (18b)$$

where $r = U_2/U_1$ and β is the angle between the transverse and streamwise components of the low-speed stream velocity vector far from the layer, i.e., $\tan \beta = V_2/U_2$, and S_{vis} is the visual thickness of the layer.⁸ See Fig. 7. Conversely, if the angles α_1 , α_2 , and β are known or can be obtained from flow visualization data, then Eq. (18) could be used to estimate the volume flux entrainment ratio.

IV. Discussion

It may be useful to consider some of the implications of the preceding arguments. The calculation of both the entrainment

ratio and the growth of the shear layer rely on an empirical datum: the local large-structure-to-position ratio ℓ/x [Eq. (11)], which experimental evidence suggests is independent of the density ratio.¹⁴ In the context of the present discussion, note that both the entrainment ratio and the growth of the shear layer would revert to the predictions for a temporally growing shear layer if $\ell/x = 0$, i.e., if the vortical structures were not large compared to x , which would result in a small upstream/downstream asymmetry. A second empirical datum is, of course, the constant ϵ that appears in Eq. (3) used in the derivation of the shear-layer growth rate.

The entrainment ratio of the spatially growing layer is given by $E = \sqrt{s} \cdot (1 + \ell/x)$. The density dependence (\sqrt{s}) is an expression for the relative induction velocity ratio of the two freestreams, as seen in the frame of the vortices [see Eq. (5)], and would also apply to a temporally growing layer, as has been argued by Brown.⁶ The second factor, however, is a statement about the large-scale structures in a spatially growing layer and describes the geometric progression of their expected locations. While the available evidence suggests that large-scale structures would also characterize a temporally growing layer, as indicated by all computational results using a variety of methods, that flow would not possess any upstream/downstream asymmetry and consequently would not be subject to the same argument. It should also be noted that, as a consequence, the induction velocity ratio for the spatially growing shear layer is not equal to the entrainment flux ratio.

From a practical standpoint, important considerations are implied by the potentially large asymmetries in entrainment. In particular, the entrainment ratio can be substantially different from unity, especially in cases of unequal densities (see Figs. 4 and 5), which are encountered in many applications, such as combustion and mixing that results from Rayleigh-Taylor unstable interfaces. In particular, in the case of chemically reacting flows, the chemical environment dictated by the fluid mechanics can be substantially different from what would be predicted by turbulence models that assume symmetric entrainment; homogeneous, isotropic eddy diffusivity; and gradient transport mixing.

Finally, it should be noted that there is evidence to suggest that the dynamics of the two-dimensional shear layer appear to depend on more than just the velocity and density ratio of the freestreams. The experiments of Batt² indicate that a half-jet ($U_2/U_1 = 0$ shear layer) with a tripped (turbulent) initial boundary layer grows *faster*, by about 30%, than a half-jet with an untripped initial boundary layer. Interestingly enough, the experiments of Browand and Latigo⁵ at a velocity ratio $U_2/U_1 = 0.18$ and of Mungal et al.²⁰ at $U_2/U_1 = 0.4$ suggest that for $U_2/U_1 \neq 0$ the shear layer grows *slower* if the high-speed boundary layers are turbulent as opposed to laminar. This behavior does not appear to be a Reynolds number effect. In all cases, the shear layer grows linearly with distance in the mean [i.e., $\delta/x \neq f(x)$], in a way that is sensitive to the initial conditions for distances downstream, which can be as large as thousands of initial momentum thicknesses. In the context of the present discussion, the vortex-spacing-to-position ratio ℓ/x and/or the constant ϵ of Eq. (3), are somehow also a function of the initial conditions in a way that is not clear at this writing.

Acknowledgments

This work was supported by the Air Force Office of Scientific Research, Contract F49620-79-0159 and Grant AFOSR-83-0213.

References

- Batchelor, G. K., "Small-Scale Variation of Convected Quantities like Temperature in Turbulent Fluid. Part 1. General Discussion and the Case of Small Conductivity," *Journal of Fluid Mechanics*, Vol. 5, 1959, pp. 113-133.

- ²Batt, R. G., "Some Measurements on the Effect of Tripping the Two-Dimensional Shear Layer," *AIAA Journal*, Vol. 13, Feb. 1975, pp. 245-247.
- ³Bernal, L. P., "The Coherent Structure of Turbulent Mixing Layers. I. Similarity of the Primary Vortex Structure, II. Secondary Streamwise Vortex Structure," Ph.D. Thesis, California Institute of Technology, Pasadena, 1981.
- ⁴Breidenthal, R. E., "Structure in Turbulent Mixing Layers and Wakes Using a Chemical Reaction," *Journal of Fluid Mechanics*, Vol. 109, 1981, pp. 1-24.
- ⁵Browand, F. K. and Latigo, B. O., "Growth of the Two-Dimensional Mixing Layer from a Turbulent and Non-Turbulent Boundary Layer," *Physics of Fluids*, Vol. 22, No. 6, 1979, pp. 1011-1019.
- ⁶Brown, G. L., "The Entrainment and Large Structure in Turbulent Mixing Layers," *Proceedings of the 5th Australasian Conference on Hydraulics and Fluid Mechanics*, 1974, pp. 352-359.
- ⁷Brown, G. L. and Rebollo, M. R., "A Small, Fast-Response Probe to Measure Composition of a Binary Gas Mixture," *AIAA Journal*, Vol. 10, May 1972, pp. 649-652.
- ⁸Brown, G. L. and Roshko, A., "On Density Effects and Large Structure in Turbulent Mixing Layers," *Journal of Fluid Mechanics*, Vol. 64, Part 4, 1974, pp. 775-816.
- ⁹Brown, J. L., "Heterogeneous Turbulent Mixing Layer Investigations Utilizing a 2-D 2-Color Laser Doppler Anemometer and a Concentration Probe," Ph.D. Thesis, University of Missouri—Columbia, 1978.
- ¹⁰Coles, D., "Prospects for Useful Research on Coherent Structure in Turbulent Shear Flow," Invited Paper, First Asian Congress of Fluid Mechanics, Bangalore, India, Dec. 8-13, 1980, *Proceedings of the Indian Academy Science (Engineering Science)*, Vol. 4, No. 2, Aug. 1981, pp. 111-127.
- ¹¹Corrsin, S. and Kistler, A. L., "Free-Stream Boundaries of Turbulent Flows," NACA R-1244, 1955.
- ¹²Dimotakis, P. E. and Brown, G. L., "The Mixing Layer at High Reynolds Number: Large-Structure Dynamics and Entrainment," *Journal of Fluid Mechanics*, Vol. 78, Pt. 3, 1976, pp. 535-560.
- ¹³Hernan, M. A. and Jimenez, J., "Computer Analysis of a High Speed Film of the Plane Mixing Layer," *Journal of Fluid Mechanics*, Vol. 119, 1982, pp. 323-345.
- ¹⁴Konrad, J. H., "An Experimental Investigation of Mixing in Two-Dimensional Turbulent Shear Flows with Applications to Diffusion-Limited Chemical Reactions," Ph.D. Thesis, California Institute of Technology, Pasadena; Project SQUID Tech. Rept. CIT-8-PU, Dec. 1976.
- ¹⁵Koochesfahani, M. M., "Experiments on Turbulent Mixing and Chemical Reactions in a Liquid Mixing Layer," Ph.D. Thesis, California Institute of Technology, Pasadena, 1984.
- ¹⁶Koochesfahani, M. M., Catherasoo, C. J., Dimotakis, P. E., Gharib, M., and Lang, D. B., "Two-Point LDV Measurements in a Plane Mixing Layer," *AIAA Journal*, Vol. 17, Dec. 1979, pp. 1347-1351.
- ¹⁷Koochesfahani, M. M. and Dimotakis, P. E., "Laser Induced Fluorescence Measurements Concentration in a Plane Mixing Layer," *AIAA Journal*, Vol. 23, Nov. 1985, pp. 1700-1707.
- ¹⁸Koochesfahani, M. M., Dimotakis, P. E., and Broadwell, J. E., "A 'Flip' Experiment in a Chemically Reacting Turbulent Mixing Layer," *AIAA Journal*, Vol. 23, Aug. 1985, pp. 1191-1194.
- ¹⁹Mungal, M. G. and Dimotakis, P. E., "Mixing and Combustion with Low Heat Release in a Turbulent Mixing Layer," *Journal of Fluid Mechanics*, Vol. 148, 1984, pp. 349-382.
- ²⁰Mungal, M. G., Dimotakis, P. E., and Hermanson, J. C., "Reynolds Number Effects on Mixing and Combustion in a Reacting Shear Layer," AIAA Paper 84-0371, Jan. 1984.
- ²¹Roshko, A., "Structure of Turbulent Shear Flows: A New Look," *AIAA Journal*, Vol. 14, Oct. 1976, pp. 1349-1357; Vol. 15, May 1977, p. 768.
- ²²Tennekes, H. and Lumley, J. L., *A First Course in Turbulence*, MIT Press, Cambridge, MA, 1972.
- ²³Townsend, A. A., "The Mechanism of Entrainment in Free Turbulent Flows," *Journal of Fluid Mechanics*, Vol. 26, Part 4, 1966, pp. 689-715.
- ²⁴Townsend, A. A., *The Structure of Turbulent Shear Flow*, 2nd ed. Cambridge University Press, New York, 1976.
- ²⁵Winant, C. D. and Browand, F. K., "Vortex Pairing: The Mechanism of Turbulent Mixing Layer Growth at Moderate Reynolds Number," *Journal of Fluid Mechanics*, Vol. 63, Part 2, 1974, pp. 237-255.
- ²⁶Wallace, A. K., "Experimental Investigation on the Effects of Chemical Heat Release in the Reacting Turbulent Plane Shear Layer," Ph. D. Thesis, University of Adelaide, 1981; AFOSR-TR-84-0650, 1984.